Recapillarity: Electrochemically Controlled Capillary Withdrawal of a Liquid Metal Alloy from Microchannels

*Mohammad R. Khan, Chris Trlica, and Michael D. Dickey**

This paper describes the mechanistic details of an electrochemical method to control the withdrawal of a liquid metal alloy, eutectic gallium indium (EGaIn), from microfluidic channels. EGaIn is one of several alloys of gallium that are liquid at room temperature and form a thin (nm scale) surface oxide that stabilizes the shape of the metal in microchannels. Applying a reductive potential to the metal removes the oxide in the presence of electrolyte and induces capillary behavior; we call this behavior "recapillarity" because of the importance of electrochemical reduction to the process. Recapillarity can repeatably toggle on and off capillary behavior by applying voltage, which is useful for controlling the withdrawal of metal from microchannels. This paper explores the mechanism of withdrawal and identifies the applied current as the key factor dictating the withdrawal velocity. Experimental observations suggest that this current may be necessary to reduce the oxide on the leading interface of the metal as well as the oxide sandwiched between the wall of the microchannel and the bulk liquid metal. The ability to control the shape and position of a metal using an applied voltage may prove useful for shape reconfigurable electronics, optics, transient circuits, and microfluidic components.

1. Introduction

The ability to accurately manipulate liquids on the sub-mm length scale is important for many applications including MEMS devices (e.g., sensors, actuators, and RF electronics), micro-total analysis systems, micropumps for mixing and analyses of fluids, reconfigurable electronics (antennas, interconnects, relays), and optics.[1–14] Metals are particularly desirable for such applications because of their optical, thermal, and electrical properties. One material that holds promise for these applications is eutectic gallium indium (EGaIn), one of several alloys of gallium that are liquid metals at room temperature.[14,15] EGaIn has a melting point of 15.7 °C[16] and a liquid phase viscosity approximately twice that of water.[17,18] It has metallic conductivity[15,19] and low toxicity,[20] making it an attractive alternative to mercury for many applications.[3,21–23]

EGaIn spontaneously forms a thin and passivating surface oxide layer at room temperature in the presence of oxygen, even at ppm O_2 levels.[24,25] Though this oxide has historically been considered a nuisance,[26,27] it provides unique opportunities to control the shape of the metal.[28] This oxide "skin" envelopes the liquid and provides mechanical stability that allows EGaIn to be molded into non-equilibrium shapes that would usually be disallowed by surface tension.[29,30] The skin has been harnessed to print the metal in 3-D[30] and 2-D[31] and to form stretchable interconnects,[32] wires,[33] antennas,[13,29] sensors,[34,35] and plasmonic structures[36] fabricated by injecting the metal into microchannels.

Because EGaIn is a liquid, its shape and position can be controlled by inducing it to flow. Injecting the metal into a microchannel is straightforward by using pressure differentials. This injection technique has been used to create shape-reconfigurable antennas and filters composed of alloys of gallium that change length in response to pressure.[37–39]

Inducing the metal to flow out of a microchannel, however, is more challenging. The presence of the oxide skin can cause the metal to leave residue on the channel walls (**Figure 1**a), like wet paint flowing through a tube.[40] It is possible to use Teflon-like surfaces or roughened surfaces[40–43] to reduce the adhesion of the metal oxide, but these approaches limit the materials of construction and increase the complexity of fabrication. It is also possible to use acid or base to remove the oxide skin, but this approach lacks external control and involves the use of possibly hazardous or corrosive materials.[44] For these reasons, most studies involving the actuation of liquid metals in microchannels focus on Hg despite its toxicity.[45–47]

The Pourbaix diagram predicts that reductive electrochemical potentials can remove the oxide skin on gallium.[48] Without the stabilizing presence of the skin, the metal undergoes capillary action to minimize its surface energy. Figure 1b (and Supporting Information Movie S1) illustrates this concept: A puddle of the metal beads up in response to a reductive potential. Although an applied bias likely lowers the interfacial tension of the metal (relative to bare metal) via electrocapillarity,[49] the tension is still large enough to induce capillary phenomena. This phenomenon can be exploited to induce withdrawal of the metal in microchannels (Figure 1c and Supporting Information Movie S2) by capillary action toward a reservoir where the metal may lower its interfacial energy by adopting a larger radius of curvature.[50] Importantly, in the absence of applied potential,

M. R. Khan, C. Trlica, Prof. M. D. Dickey
Department of Chemical & Biomolecular Engineering
North Carolina State University
Raleigh, NC 27607, USA
E-mail: mddickey@ncsu.edu

DOI: 10.1002/adfm.201403042

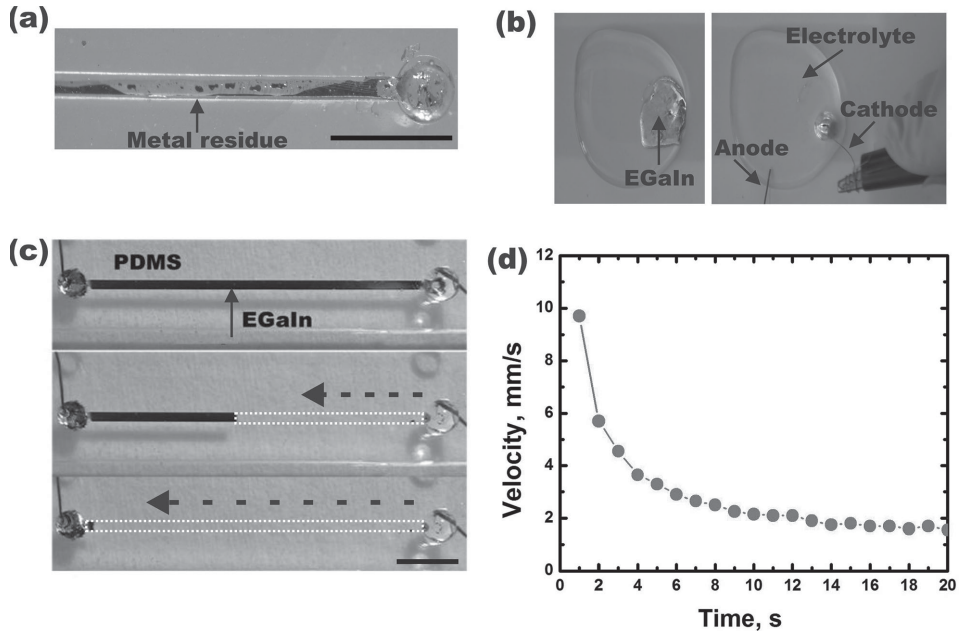

Figure 1. a) Photograph of metal residue on the sidewalls of polydimethylsiloxane (PDMS) microchannels after attempting to withdraw EGaIn using pneumatics. b) The oxide skin stabilizes the shape of a puddle of metal submerged in electrolyte. Application of a reductive potential to the metal removes the oxide and the high surface tension of the metal causes it to bead up. c) An example of reduction-driven liquid metal withdrawal in a PDMS microchannel. The EGaIn cathode connects electrically to a counter electrode by a dilute salt solution (10 mM NaF). A reductive potential (1 V) applied to the liquid metal causes it to withdraw from the microchannel toward a reservoir, leaving the capillary filled with electrolyte. d) A characteristic plot of the velocity of liquid metal withdrawal over time. (Both scale bars are 5 mm).

the skin rapidly reforms, allowing capillary flow to be stopped on demand. Controlling interfacial phenomena represents an attractive way to manipulate fluids since capillary forces dominate on the sub-mm length scale.[51,52] Furthermore, the use of applied voltage is an ideal way to manipulate fluids because it is highly controllable, easily accessible, and does not require bulky or moving parts.[53–56]

We call the technique "recapillarity" because it uses reduction to induce capillarity. The term also refers to the ability to repeatedly turn on and off the capillary behavior. Recapillarity is an attractive alternative to conventional electrohydrodynamic approaches for manipulating fluids (e.g., electroosmosis, electrowetting),[57] which are difficult to implement with EGaIn for a number of reasons including the large yield stress of the oxide skin.[14] In contrast, recapillarity takes advantage of the skin by removing it on demand. Here, we describe the velocity of the withdrawal of EGaIn from microchannels induced by recapillarity, characterize the role various experimental parameters play on the withdrawal, and propose a mechanism to explain the withdrawal. The proposed mechanism implies that oxide is present between the metal and the walls of the channel, which is otherwise a difficult interface to probe.

2. Results and Discussion

To study withdrawal induced by recapillarity, we used an inert acrylic platform with two reservoirs for holding liquid, bridged by a glass capillary (depicted in Supporting Information, Figure S1). Electrodes connected the fluid in each reservoir to a voltage source (Pine WaveNow AFTP1 potentiostat). An electrolyte (10 mM NaF) filled one reservoir and EGaIn filled the other. Capillaries pre-filled with liquid metal spanned the apparatus horizontally such that each end remained immersed in a reservoir, completing the circuit. Straight borosilicate capillaries (0.9 ± 0.1 mm inner diameter, 70 mm long) are well-suited for these experiments because they are inexpensive, optically transparent, and oxygen impermeable. They also have round cross-sections and thus lack sharp corners that could create void space.

Upon applying a reductive potential, the liquid metal withdraws from microchannels at a velocity that decays over time, as shown in Figure 1d. Regardless of the absolute velocity, withdrawal velocities start high and then decay. This holds for all of the constant-voltage experimental conditions we explored, including a range of salt concentrations (1 μM to 3 M), applied voltages (100 mV to 4 V), and capillary tube diameters (0.25 mm to 1 mm inner diameter). We sought to understand the behavior of this system by studying the parameters that could impact the rate of withdrawal.

Unless otherwise noted, 10 mM NaF was used as the electrolyte (though all the electrolytes we tried produced similar results). More concentrated electrolytes result in withdrawal velocities that are too fast to observe easily; remarkably, 1 M NaF at 1 V causes the metal to withdraw at a maximum velocity of ≈10–30 cm/s (Supporting Information, Figure S2). Supporting Information Movie S3 demonstrates a fast withdrawal using 0.1 M NaF and Movie S4 demonstrates a comparatively slower withdrawal using 10 mM NaF for otherwise identical experimental conditions.

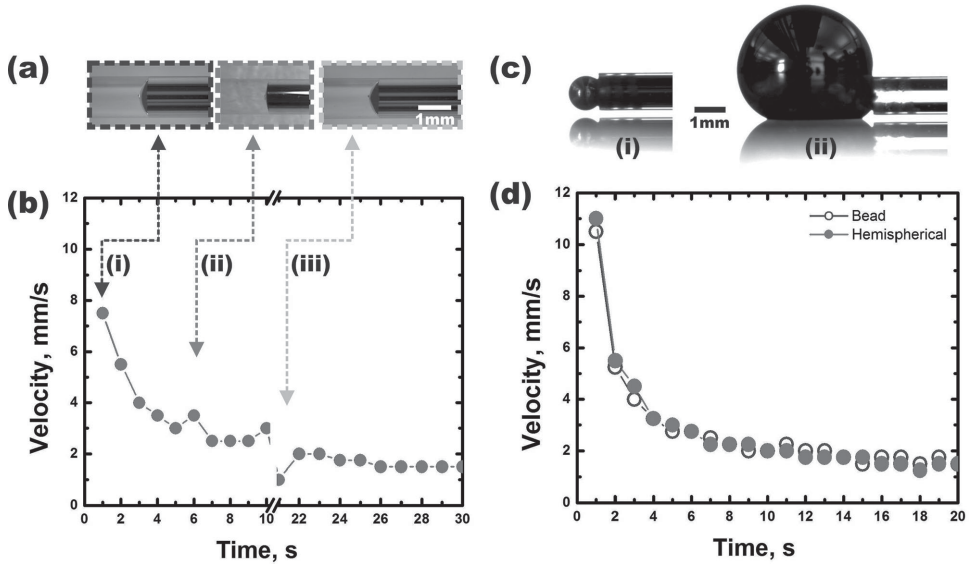

Figure 2. Effect of a,b) meniscus shape and c,d) shape of the metal in the reservoir on withdrawal velocity. a) Top down photographs (i–iii) of liquid metal menisci. At the beginning of the experiment, i) a hemispherical meniscus ii) flattens out during recapillarity, and then iii) returns to an equilibrium hemispherical shape in the absence of voltage. b) Plot of velocity versus time to test the effect of meniscus shape. After 10 s, withdrawal stops when the applied voltage is zero. Ten seconds later, after the meniscus has re-equilibrated, withdrawal continues by re-application of the voltage with no appreciable change in velocity (at $t = 22$ s). c) Side view of two end reservoirs over time including one in the shape of i) a small bead and ii) a large hemisphere. d) Plot of the velocity with metal reservoirs of different shape and size, showing that geometry of the metal does not have a significant effect on metal withdrawal.

There are a number of possible factors contributing to the decay in the withdrawal velocity. Since capillary forces are often important on the sub-mm length scale, we examined potential interfacial factors in addition to electrochemical factors. We examined: 1) the shape of the liquid metal meniscus as the metal retreats from the channel; 2) the size and shape of the metal in the reservoir; 3) possible ion gradients at the EGaIn/electrolyte interface; 4) effects of physical channel geometry such as length; and 5) electrical path length. After systematically studying each of these parameters, we show that the only variables significantly influencing withdrawal velocity are those affecting the applied current.

2.1. Meniscus Shape

At rest, the metal plug in the capillary adopts a hemispherical meniscus at the electrolyte interface, as shown in **Figure 2**a,i. However, during withdrawal, the meniscus flattens (cf., Figure 2a,ii). We hypothesized that this change in the meniscus shape lowers the withdrawal velocity relative to a curved meniscus since a flat meniscus would have a lower capillary pressure and therefore a smaller driving force for withdrawal. To test this hypothesis, we used recapillarity to withdraw the liquid metal halfway along the length of the glass capillary. In the absence of potential, the metal stops moving and the meniscus equilibrates to a round shape within ≈100 μs (Figure 2a,iii). The round shape of the meniscus at equilibrium is similar to its shape prior to starting the experiment. Applying a reductive potential again (at 21 s in Figure 2b) causes the metal to begin withdrawing again, continuing at a similar velocity as before the voltage ceased. Since the velocity did not increase after allowing the meniscus to re-equilibrate, we rejected this hypothesis. We will later show that the shape of the meniscus is a consequence of the withdrawal mechanism.

2.2. Shape of the Metal Reservoir

As the metal flows out of the capillary into the reservoir, the reservoir increases in volume. We speculated that the capillary pressure at the receiving reservoir might affect the withdrawal velocity, although in principle, the pressure opposing recapillarity should decrease as the reservoir inflates with more metal and therefore allow the withdrawal velocity to increase with time. We varied the amount of metal at the reservoir to change its shape from a small bead (i.e., bead diameter approximately equal to tube diameter) to a much larger drop (i.e., diameter two or more times larger than the tube diameter), as shown in Figure 2c. The withdrawal velocities were nearly identical in both cases (Figure 2d), suggesting that withdrawal velocities are independent of reservoir size and shape for the range of length scales explored in the experiments described in this paper. Later we show that electrochemical processes dictate the velocity of withdrawal.

2.3. Ion Gradients

Because electrochemical reactions drive the withdrawal process, we hypothesized that local changes in the concentration of ion species (e.g., Ga^{+3}, OH^-, H^+, Na^+, F^-) near the liquid metal interface may affect the withdrawal. After withdrawing the metal partially, we turned off the applied voltage. We waited

for ≈10–20 s to let the meniscus recover its shape, that is, a flat meniscus returns back to hemispherical shape (cf., Figure 2a,i). Then we refreshed the electrolyte/metal oxide interface by inserting a syringe needle (Supporting Information, Figure S3a) into the capillary tube and gently flushing the interface with fresh electrolyte. Figure S3b shows that after re-initiating withdrawal, there is no increase in velocity, suggesting that ion gradients do not significantly affect the withdrawal velocity.

2.4. Liquid Displacement

As metal withdraws from the capillary it simultaneously pulls electrolyte into the capillary. The viscosity of the electrolyte is lower than that of the metal, so it should not reduce the speed of withdrawal. Our results suggest a more dominant effect is the change in electrical resistance along the long axis of the tube. Electrolyte replaces the metal as it withdraws, lengthening the electrical path between the two electrodes. We therefore hypothesized that the increasing electrical distance between the liquid metal surface and the counter-electrode causes the decay in velocity. To test this hypothesis, we withdrew the metal halfway out of the capillary and then turned off the voltage. Inserting the counter-electrode into the capillary (Supporting Information, Figure S4) returned the electrode-electrode distance to a value similar to that at the beginning of the experiment. After re-initiating withdrawal by application of potential, the velocity began high and subsequently decayed, mimicking the decay observed during the first portion of the experiment, as seen in **Figure 3**a. This result supports the hypothesis that the electrical length causes the decay of the withdrawal velocity. As a complementary experiment, we reversed the direction of flow by using a syringe pump to physically force metal into an electrolyte-filled capillary while measuring the amperometric behavior. In principle, as the electrolyte gets displaced by metal, the electrical resistance should decrease through the capillary. Consistent with our hypothesis, the current increases as EGaIn displaces the solution (Supporting Information, Figure S5). Likewise, physically obstructing the withdrawal during recapillarity results in constant current.

Given these results, we sought a mechanism to relate current to velocity. As the metal withdraws, the electrical length between the two electrodes increases and current decreases. The current decreases proportional to velocity, as shown in Figure 3a. Figure 3b shows that current scales inversely with length (i.e., the length of the electrolyte in the capillary), as expected for a system following Ohm's law. Figure 3c shows that it is possible to attain constant withdrawal velocity by applying a constant current (≈20 μA). These results illustrate the importance of current, but they do not explain why current is necessary.

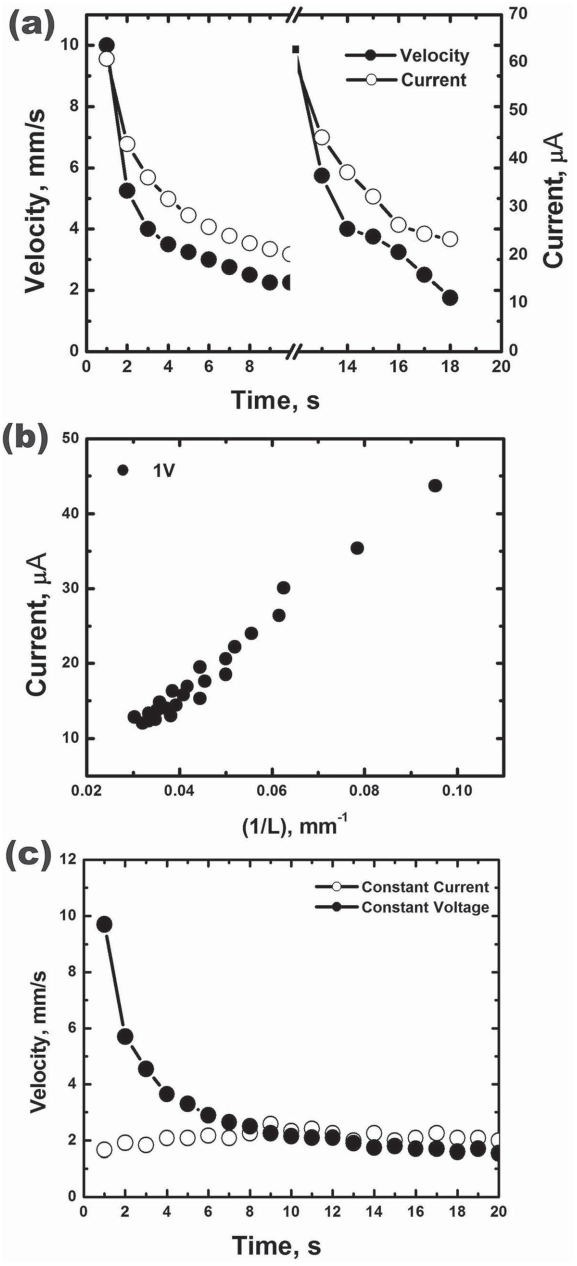

Figure 3. Effect of electrical length on the liquid metal withdrawal. a) After withdrawing the metal for 10 s but before starting the second withdrawal, a copper wire (anode) inserted into the capillary shortens the electrical distance between the anode and the metal interface. We do not show the time spent inserting the electrode on the time axis. Restarting the withdrawal by application of a reductive potential (t = 13 s) to the liquid metal causes the velocity and current to mimic both the starting magnitude and decay profile of the initial withdrawal. b) Plot of measured current versus inverse length of partially withdrawn metal yields a nearly linear relationship; linear best fit R^2 = 0.97. c) A recapillarity experiment performed at constant current rather than constant voltage results in a nearly constant withdrawal velocity.

2.5. Electro-osmotic Effects

First, electro-osmotic flow is a sensible consideration for fluid motion in a system driven by current. For several reasons, we reject electroosmosis as a primary driving force in this system. Appreciable electro-osmotic flow in DC systems usually requires high electric field strength; the electric field in this system is quite weak (≈0.014 V/mm) and increasing field strength does not proportionally increase flow velocity. The

maximum electro-osmotic flow rates demonstrated in the literature are on the order of mm/s,[51] whereas we observe velocities of tens of cm/s. Finally, electro-osmotic mobility declines with increasing electrolyte concentration and we observe greatly increased flow velocities at higher electrolyte concentrations (cf. Supporting Information Figure S2).

2.6. Electrochemical Effects and Meniscus Analysis

The dependence of withdrawal velocity on current is intuitive in the sense that the electrochemical reduction of the oxide necessitates current (i.e., Faradaic processes must occur), but it is less obvious why current must be applied throughout the withdrawal. We initially expected that the current would remove the hemispherical oxide "cap" that separates the metal and the solution, but in that case, the withdrawal should be approximately constant after an initial transient and show a dependence on the radii of curvature of both the meniscus and the reservoir. The need for continual current suggests that oxide must be removed continually.

The shape of the meniscus and velocity during the withdrawal provides some insight into the withdrawal mechanism. The four columns in **Figure 4** represent different approaches for inducing withdrawal. All of the experiments begin with an empty capillary (Figure 4a–c) except those depicted in Figure 4d, which begin with a capillary prefilled with 1 M HCl. After injecting the metal into these capillaries, the metal assumes a hemispherical profile at rest (cf. Figure 2a,i). An oxide layer coats the hemispherical cap due to its contact with air. We also depict an oxide layer separating the metal from the capillary walls to help explain our interpretation of the withdrawal mechanism. Due to the presence of the oxide, the metal does not withdraw spontaneously from the capillaries. In contrast, Figure 4d shows that the presence of acid during injection keeps the metal oxide-free and the metal withdraws spontaneously (Supporting Information Movie S5) and rapidly (≈30–40 cm/s) with a rounded meniscus the entire time.

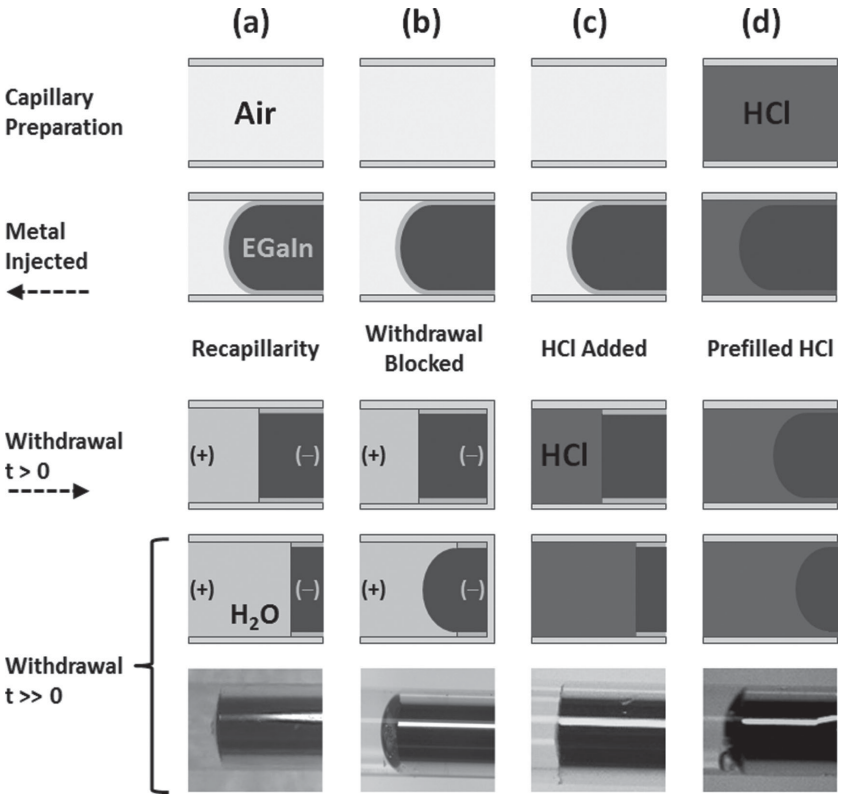

Figure 4. The shape of the meniscus during withdrawal provides mechanistic insight into recapillarity. The four columns correspond to four unique experiments. In columns)a–c) metal is injected right-to-left into an empty capillary tube, followed by addition of electrolyte. In column (d), the metal is injected into a capillary prefilled with 1 M HCl. In all cases, the meniscus is hemispherical after injection. a) The meniscus is nearly flat during recapillarity (withdrawing left to right). b) The capillary is physically blocked to keep the metal from withdrawing. Application of a reductive potential removes the oxide on the cap of the meniscus, and it begins to become round as the oxide is etched away from the wall. c) The meniscus is also flat when withdrawal is induced by adding acid to the end of a capillary prefilled with metal (no voltage). d) The meniscus is round when the metal withdraws spontaneously (no voltage) from a capillary prefilled with acid.

Figure 4a shows the shape of the meniscus during recapillarity (Supporting Information Movie S4). The metal-electrolyte interface flattens (i.e., large radius of curvature), which is unexpected based on the large surface tension of the bare metal. We refer to the shape of the meniscus as flat but note that the opaque nature of the metal makes it difficult to determine the exact shape.

In a seperate experiment, we blocked the outlet of the capillary to hinder the withdrawal (Figure 4b and Supporting Information Movie S6). The small pressure from injecting water via a syringe needle into the capillary causes the oxide-coated meniscus to artificially flatten prior to applying potential. This flattened meniscus is apparent at the onset of Movie S6. Upon application of a reductive potential, the metal does not withdraw because it is physically obstructed. The shape of the meniscus, however, slowly becomes more round, as shown in Figure 4b, which suggests the metal slowly pulls away from the wall over time and that reduction of oxide along the wall may be occurring.

We also observed a flat meniscus while inducing the withdrawal by the addition of 10 mM acid after pre-filling an empty capillary with metal, as shown in Figure 4c (Supporting Movie S7). The acid causes the metal to withdraw in the absence of potential. If the oxide coated only the meniscus of the metal, then removing it via acid should cause rapid withdrawal. Instead, the withdrawal velocity is relatively slow (≈3–4 mm/min) compared to that obtained with a channel pre-filled with acid. The similarity of the shape of the menisci in Figure 4a,c suggests that electrocapillarity is not a primary cause of the shape of the meniscus observed during recapillarity.[49]

These results, taken in sum, suggest that 1) there is oxide between the walls of the capillary and the metal, 2) upon removal of the oxide on the meniscus, the resulting bare metal wets the remaining oxide on the walls to create a non-hemispherical meniscus, and 3) the reduction of the oxide on the walls limits the rate of withdrawal and may explain why the withdrawal velocity correlates only with applied current.

If there is an oxide between the metal and the walls of the capillary, then it likely forms during injection since the capillary walls are impermeable to oxygen. We speculate that the oxide layer on the leading meniscus of the metal adheres to the walls during injection and a new oxide reforms rapidly and repeatedly shears off as the metal fills the channel.

We performed an additional experiment to test for consistency of the presence of oxide between the metal and the walls of the channel. If this oxide layer exists, the withdrawal velocity during recapillarity should scale with radius rather than cross-sectional area of the capillary (for a given current) since the oxide surrounds the circumference of the metal plug. Using the conditions found in Figure 3c, we compared the withdrawal velocity at constant current (20 μA) for capillaries with small (260 μm) and large (1 mm) inner diameters, and found average withdrawal velocities of 3.8 mm/s and 2 mm/s, respectively, over a withdrawal distance of 4 cm. The ratio of withdrawal velocity (1:2) is much closer to scaling with perimeter (1:4) rather than cross sectional area (1:16). There are complications that come with such comparisons, however. First, a decrease in capillary diameter corresponds not only to a decrease in the circumferential length of the oxide but also to changes in viscous drag. Second, applying a constant current can also cause a fluctuation in voltage, which can lead to electrochemical reactions other than reduction of the oxide that contribute to the current but do not influence the velocity. We are currently working to understand these subtleties.

2.7. Demonstration

It is possible to use recapillarity to withdraw the metal along arbitrary paths by maintaining an electrically connected pathway. We created a complex metal shape to illustrate the ability to induce withdrawal of the metal along specific paths on demand. For example, **Figure 5**a–d shows that by arbitrarily switching the position of the electrodes, the directionality of withdrawal can be controlled to reconfigure the shape of the liquid metal. This concept can also be applied to a much more complicated microfluidic network of liquid metal microstructures as shown in Figure 5e,f (Supporting Information Movie S8). The results of Figure 5f suggest that recapillarity enables fluids to "solve" complex mazes by withdrawing along the shortest electrical path.

3. Conclusion

We demonstrate a simple approach to turn on and off capillary behavior of a liquid metal in microchannels, exploiting the reduction of a thin gallium oxide layer that forms spontaneously on EGaIn. Flow can be stopped or started arbitrarily using low voltages (≈1 V), withdrawal speed can be controllably varied up to 30 cm/s, and the metal can withdraw selectively along complex paths with minimal disturbance to neighboring metal traces. Current-limiting effects, such as electrolyte concentration and electrical path length, are the most important factors governing the rate of withdrawal of the liquid metal. We speculate that this withdrawal requires current because of the need to continually reduce the thin oxide layer. The results suggest further that in addition to forming a cap on the meniscus of the metal, an oxide layer likely exists sandwiched between the bulk liquid metal and the sidewall of the capillary,

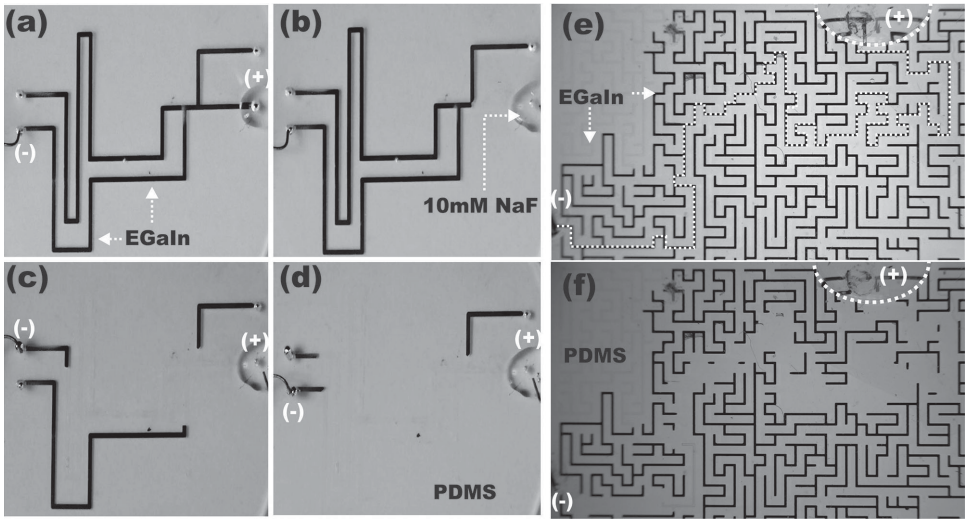

Figure 5. Two demonstrations of shape-reconfigurability of liquid metal microstructures by recapillarity. a) A microfluidic channel of arbitrary shape is filled with liquid metal that is mechanically stabilized by its oxide skin. 10 mM NaF is added as working electrolyte and copper electrodes are attached to the inlet and outlet. b) Applying ≈40 μA reductive current induces withdrawal. c,d) Switching the position of the active electrode controls the withdrawal path. The withdrawal can be halted at any time by turning off the voltage. Only the metal in the electrical path withdraws when the voltage is turned on. e,f) Withdrawal of liquid metal from a maze-shaped array of microchannels. The dotted line as shown in (e) is the only electrically connected path through which the metal can be withdrawn. f) Application of 40 μA induces withdrawal. Only the metal along the electrical path flows out of the device.

which may further explain why current is needed throughout the withdrawal process and why the meniscus flattens during withdrawal.

Recapillarity has several limitations. First, it requires electrolyte. Second, high withdrawal velocities require large applied currents, but large currents in dilute electrolytes may necessitate voltages exceeding the electrolysis voltage of water. Bubbles can disrupt the electrical circuit required to induce withdrawal of the metal; although this was not a serious issue for the conditions used in this paper, it could pose problems for some applications. Finally, recapillarity induces capillary behavior, which implies that the metal will only flow in directions that lower the total interfacial energy.

Nevertheless, the ability to electrically control the position and velocity—and therefore the shape—of a liquid metal in microchannels is a promising development in the realization of a number of novel applications such as reconfigurable wires, antennas, sensors, actuators, soft robots, meta-materials, plasmonics, transient circuits, and micro pumps.

4. Experimental Section

An HD camcorder (Canon VIXIA HF S20) mounted on a microscope (Olympus SZ-61) recorded the withdrawal. When needed, a high speed camera replaced the camcorder to capture higher frames per second. The withdrawal velocity data were extracted by analyzing the position of the metal in each video.

Acknowledgements

The authors acknowledge support from NSF CAREER (CMMI-0954321) and Samsung.

Received: September 3, 2014
Revised: October 12, 2014
Published online: November 19, 2014

[1] P. Gravesen, J. Branebjerg, O. S. Jensen, *J. Micromech. Microeng.* **1993**, *3*, 168.
[2] B. Zhao, J. S. Moore, D. J. Beebe, *Science* **2001**, *291*, 1023.
[3] P. Sen, C.-J. Kim, *J. Microelectromech. Syst.* **2009**, *18*, 174.
[4] R. Shabani, H. J. Cho, *Sens. Actuators B: Chem.* **2013**, *180*, 114.
[5] B. S. Gallardo, V. K. Gupta, F. D. Eagerton, L. I. Jong, V. S. Craig, R. R. Shah, N. L. Abbott, *Science* **1999**, *283*, 57.
[6] H. A. Stone, A. D. Stroock, A. Ajdari, *Annu. Rev. Fluid Mech.* **2004**, *36*, 381.
[7] C. S. Zhang, D. Xing, Y. Y. Li, *Biotechnol. Adv.* **2007**, *25*, 483.
[8] P. Sen, C.-J. Kim, *IEEE Trans. Ind. Electron.* **2009**, *56*, 1314.
[9] Z. Nie, C. A. Nijhuis, J. Gong, X. Chen, A. Kumachev, A. W. Martinez, M. Narovlyansky, G. M. Whitesides, *Lab Chip* **2010**, *10*, 477.
[10] S.-Y. Tang, V. Sivan, K. Khoshmanesh, A. P. O'Mullane, X. Tang, B. Gol, N. Eshtiaghi, F. Lieder, P. Petersen, A. Mitchell, K. Kalantar-zadeh, *Nanoscale* **2013**, *5*, 5949.
[11] C.-M. Ho, Y.-C. Tai, *Annu. Rev. Fluid Mech.* **1998**, *30*, 579.
[12] V. Hessel, H. Löwe, F. Schönfeld, *Chem. Eng. Sci.* **2005**, *60*, 2479.
[13] S. Cheng, Z. Wu, *Lab. Chip* **2010**, *10*, 3227.
[14] M. D. Dickey, R. C. Chiechi, R. J. Larsen, E. A. Weiss, D. A. Weitz, G. M. Whitesides, *Adv. Funct. Mater.* **2008**, *18*, 1097.
[15] R. C. Chiechi, E. A. Weiss, M. D. Dickey, G. M. Whitesides, *Angew. Chem. Int. Ed.* **2008**, *47*, 142.
[16] S. J. French, D. J. Saunders, G. W. Ingle, *J. Phys. Chem.* **2002**, *42*, 265.
[17] K. E. Spells, *Proc. Phys. Soc. Lond.* **1936**, *48*, 299.
[18] J. N. Koster, *Cryst. Res. Technol.* **1999**, *34*, 1129.
[19] D. Zrnic, D. S. Swatik, *J. Common Met.* **1969**, *18*, 67.
[20] CRC Handbook of Chemistry and Physics, 92nd Edition, CRC Press, Boca Raton **2011–2012**.
[21] K.-S. Yun, I.-J. Cho, J.-U. Bu, C.-J. Kim, E. Yoon, *J. Microelectromech. Syst.* **2002**, *11*, 454.
[22] S. Arscott, M. Gaudet, *Appl. Phys. Lett.* **2013**, *103*, 074104.
[23] B. L. Cumby, G. J. Hayes, M. D. Dickey, R. S. Justice, C. E. Tabor, J. C. Heikenfeld, *Appl. Phys. Lett.* **2012**, *101*, 174102.
[24] M. J. Regan, H. Tostmann, P. S. Pershan, O. M. Magnussen, E. DiMasi, B. M. Ocko, M. Deutsch, *Phys. Rev. B Condensed Matter* **1997**, *55*, 10786.
[25] L. Cademartiri, M. M. Thuo, C. A. Nijhuis, W. F. Reus, S. Tricard, J. R. Barber, R. N. S. Sodhi, P. Brodersen, C. Kim, R. C. Chiechi, G. M. Whitesides, *J. Phys. Chem. C* **2012**, *116*, 10848.
[26] P. A. Giguere, D. Lamontagne, *Science* **1954**, *120*, 390.
[27] W. Shen, R. T. Edwards, C.-J. Kim, *J. Microelectromech. Syst.* **2006**, *15*, 879.
[28] M. D. Dickey, *ACS Appl. Mater. Interfaces* **2014**, DOI: 10.1021/am5043017.
[29] J. H. So, J. Thelen, A. Qusba, G. J. Hayes, G. Lazzi, M. D. Dickey, *Adv. Funct. Mater.* **2009**, *19*, 3632.
[30] C. Ladd, J.-H. So, J. Muth, M. D. Dickey, *Adv. Mater.* **2013**, *25*, 5081.
[31] J. W. Boley, E. L. White, G. T.-C. Chiu, R. K. Kramer, *Adv. Funct. Mater.* **2014**, *24*, 3501.
[32] H.-J. Kim, C. Son, B. Ziaie, *Appl. Phys. Lett.* **2008**, *92*, 011904.
[33] S. Zhu, J.-H. So, R. Mays, S. Desai, W. R. Barnes, B. Pourdeyhimi, M. D. Dickey, *Adv. Funct. Mater.* **2013**, *23*, 2308.
[34] C. Majidi, R. Kramer, R. J. Wood, *Smart Mater. Struct.* **2011**, *20*, 105017.
[35] C. Majidi, R. J. Wood, *Appl. Phys. Lett.* **2010**, *97*, 164104.
[36] J. Wang, S. Liu, Z. V. Vardeny, A. Nahata, *Opt. Express* **2012**, *20*, 2346.
[37] M. R. Khan, G. J. Hayes, J.-H. So, G. Lazzi, M. D. Dickey, *Appl. Phys. Lett.* **2011**, *99*, 013501.
[38] M. R. Khan, G. J. Hayes, S. Zhang, M. D. Dickey, G. Lazzi, *IEEE Microw. Wirel. Compon. Lett.* **2012**, *22*, 577.
[39] J. Wang, S. Liu, S. Guruswamy, A. Nahata, *Appl. Phys. Lett.* **2013**, *103*, 221116.
[40] R. K. Kramer, J. W. Boley, H. A. Stone, J. C. Weaver, R. J. Wood, *Langmuir*, **2014**, *30*, 533.
[41] D. Kim, D.-W. Lee, W. Choi, J.-B. Lee, *J. Microelectromech. Syst.***2013**,*22*,1267.
[42] D. Kim, D. Jung, J. H. Yoo, Y. Lee, W. Choi, G. S. Lee, K. Yoo, J.-B. Lee, *J. Micromech. Microeng.* **2014**, *24*, 055018.
[43] K. Doudrick, S. Liu, E. M. Mutunga, K. L. Klein, V. Damle, K. K. Varanasi, K. Rykaczewski, *Langmuir* **2014**, *30*, 6867.
[44] G. Li, M. Parmar, D. Kim, J.-B. (JB) Lee, D.-W. Lee, *Lab. Chip* **2013**, *14*, 200.
[45] J. L. Jackel, S. Hackwood, G. Beni, *Appl. Phys. Lett.* **1982**, *40*, 4.
[46] G. Maltezos, R. Nortrup, S. Jeon, J. Zaumseil, J. A. Rogers, *Appl. Phys. Lett.* **2003**, *83*, 2067.
[47] D. Rodrigo, L. Jofre, B. A. Cetiner, *IEEE Trans. Antennas Propag.* **2012**, *60*, 1796.
[48] M. Pourbaix, *Atlas of Electrochemical Equilibria in Aqueous Solutions*, Second English Edition., Vol. 16.1, Natl. Assn. of Corrosion, TX, USA **1974**.

[49] A. Frumkin, N. Polianovskaya, N. Grigoryev, I. Bagotskaya, *Electrochim. Acta* **1965**, *10*, 793.
[50] M. Khan, C. Eaker, E. Bowden, M. Dickey, *Proc. Natl. Acad. Sci.* **2014**, *111*, 14047.
[51] A. Castellanos, *Electrohydrodynamics*, Springer, New York **1998**.
[52] P. Tabeling, *Introduction to Microfluidics*, Reprint.; Oxford University Press, USA **2010**.
[53] F. Mugele, J.-C. Baret, *J. Phys. Condens. Matter* **2005**, *17*, R705.
[54] V. Sivan, S.-Y. Tang, A. P. O'Mullane, P. Petersen, N. Eshtiaghi, K. Kalantar-zadeh, A. Mitchell, *Adv. Funct. Mater.* **2013**, *23*, 144.
[55] S.-Y. Tang, K. Khoshmanesh, V. Sivan, P. Petersen, A. P. O'Mullane, D. Abbott, A. Mitchell, K. Kalantar-zadeh, *Proc. Natl. Acad. Sci.* **2014**, *111*, 3304.
[56] J. T. H. Tsai, C.-M. Ho, F.-C. Wang, C.-T. Liang, *Appl. Phys. Lett.* **2009**, *95*, 251110.
[57] Z. Wan, H. Zeng, A. Feinerman, *Appl. Phys. Lett.* **2006**, *89*, 201107.